# Study of Change in Resonance Characteristics for a Passive Bimorph Damper

[1]SHANKER GANESH KRISHNAMOORTHY, [2]INGA SKIEDRAITE, [3]SYLVESTER SEDEM DJOKOTO, [4]EGIDIJUS DRAGASIUS, [5] RAMUNAS SKVIRECKAS
Faculty of Mechanical Engineering and Design
Kaunas University of Technology
Studentu Str. 56, Kaunas, LT–51424
LITHUANIA
[1]shanker.krishnamoorthy@ktu.edu, [2]inga.skiedraite@ktu.lt, [3]sylvester.djokoto@ktu.edu
[4]egidijus.dragasius@ktu.lt, [5]ramunas.skvireckas@ktu.lt

*Abstract*: Piezo materials are widely used as dampers in smart systems due to their unique properties. Several research was developed to understand the damping process strategy in piezoelectric dampers, but by giving less consideration to the effect of directly shorting terminals between passive and active layers. This research work aims to study the influence of shorting terminals of passive and active layers at the time of resonance. Simple bimorph cantilever was used for the research study to illustrate the effectiveness of the proposed technique. The experiment setup consists of input unit (wave generator amplifier, and shaker), and output unit (optical sensor, vibrometer, picoscope, and computer). The *PicoScope* software was used to analyze the final result. The results show that the new approach has a positive effect, where the amplitude of vibration at resonance can be reduced up to 50 %.

*Key-Words:* Bimorph, piezoelectric damper, shunt damping, resonance damping, passive damping, active damping.

## 1 Introduction

Piezoelectric materials are widely used in multimodal vibration damping [1] and resonant damping [2-6]. Unique properties of piezoelectric materials make it easy to install, operate, and maintain it as a resonance damper. The piezoelectric patches used for damping, will not be sized, to actuate the structure nor significantly change the stiffness of the structure to which it is attached. Thus piezoelectric dampers can be tuned to remove energy at time of resonance, which results in reduced vibration amplitude.

Mechanical vibration can be dissipated through an active or passive technique and also by combination of both. The active technique consists of power supplies and control system, where as in a passive technique the physical characteristic of smart materials determines the nature of damping [1].

The passive damping can be classified as structural and embedded damping. Damping obtained by friction of junctions, cable rubbing and material damping are categorized as structural damping. Embedded damping is achieved by adding dissipation mechanism like: viscoelastic materials, viscous devices, magnetic devices and passive piezoelectric [1].

Existing research [1] focus on study of passive damping systems for single mode or multiple modes, where damping is achieved through piezoelectric patches and resonant shunt circuits. Later this work is followed by discussion of modelling of piezoelectric patches coupled to shunt circuits involving series and parallel connections. In other research works [2-6] a combination of analytical and experimental study was done to evaluate the feasibility of passive and active approaches to reduce high cycle fatigue in turbine engine fan, compressor blades and also on other mechanical structures.

Based on the shunt circuits the piezoelectric dampers can be classified as [1, 2]:

1. resistive – here the system behaves similar to viscoelastically damped systems;
2. resonant – the system is similar to classical dynamic vibration absorber;
3. capacitive – circuit changes the stiffness of piezoelectric element;

4. switched – there the behaviour of the circuit in response can be adjusted with respect to change in system.

The changes in resonance characteristics for a bimorph cantilever setup, when the active-layer terminals and passive-layer terminals of a bimorph are shorted to one another without any shunt circuit or an external power amplifier, are investigated in this paper.

## 2 Electromechanical Characteristics of Piezoelectric Damper

The piezoelectric effect enables to transform a portion of mechanical energy associated with vibration, to electrical energy. The electrical energy can be dissipated conveniently through a shunt circuit [2-6].

The study of transient dynamic characteristics of a PZT (Lead zirconate titanate) bender can be performed using an electrical equivalent circuit. Electrical equivalent circuit has been used in previous research [9-10]. The voltage value obtained for various conditions of mechanical stress were fairly accurate. The understanding of an electrical equivalent circuit is necessary to obtain the voltage to strain relationship.

Figure 1 shows a circuit diagram for PZT beam, which consist of a mechanical and an electrical part. The mechanical part consists of a voltage source *AC*, which is connected in series with an inductor $L_m$, a resistor *R* and a capacitor $C_k$. Whereas the electrical part which represents inherent capacitance of the device consist of a capacitor $C_b$. The voltage adaptation between mechanical and electrical parts is done by a transformer *n*.

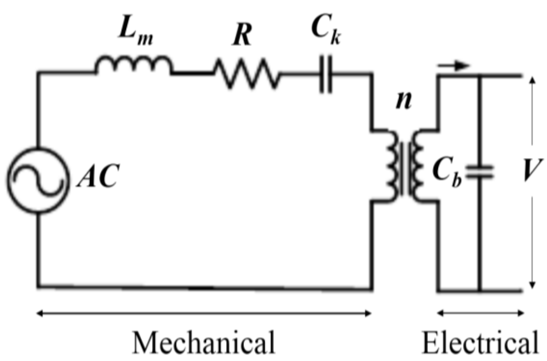


Fig 1 Circuit diagram for PZT beam

Kirchhoff's voltage law can be used to describe the above mentioned circuit (Fig.1), where the relation between strain $\varepsilon$ and voltage *V* can be expressed as [10]:

$$V = \frac{n_p t_c d_{31} Y}{\varepsilon} \dot{\varepsilon} ; \quad (1)$$

where: $\varepsilon$ is the strain, $\dot{\varepsilon}$ is the first time derivative of strain, $n_p$ describes the voltage adaptation constant, $t_c$ defines the thickness of piezo layers and also the thickness of centre shim separating the piezo layers, $d_{31}$ – the transverse piezoelectric coupling coefficient, *Y* – Young's modulus of elasticity.

For a piezoelectric material, the dielectric constant varies with mechanical load and the Young's modulus varies with electrical load. Thus, the mechanical stiffness of the material reduces when the outputs are electrically shorted. Here the efficiency of energy conversion from electrical to mechanical load can be evaluated using a factor known as electromechanical coupling factor *k*. The relation between change in stiffness of piezoelectric material when the terminals are electrically shorted can be defined using [7-8]:

$$Y_{OPEN} (1\text{-}k^2) = Y_{SHORT} \quad (2)$$

where $Y_{OPEN}$ and $Y_{SHORT}$ are the value of Young's modules of piezoelectric material for an open circuit and shorted circuit respectively. Here electromechanical coupling factor *k* is given by the ratio of electrical energy converted to mechanical displacement $E_M$ to electrical energy input *EEI* [7-8]:

$$k^2 = E_M / EEI \quad (3)$$

## 3 Mathematical Expressions for Piezoelectric Shunt Dampers

A piezoelectric material with complex stiffness, which describes the mechanism of piezoelectric dampers, can be evaluated using the energy consumption ratio and damping factor from a phase angle diagram corresponding to its real and imaginary parts. The phase angle varies depending on frequency, electrical impedance of the shunted circuit, and the properties of the piezoelectric material. Thus, the damping factor and effective stiffness of the damper are controllable by adjusting the frequency and electrical impedance [11].

Damping factor $\beta$ can be explained using complex stiffness matrix ${}^{RE}Y$ of a piezoelectric damper. Piezoelectric shunt damper connected with impedance *Z* and vibrating in direction *1* is shown in Fig. 2. The impedance is treated as piezoelectric material with overall impedance ${}^{RE}Z$ (3x3 components). If there is no external electrical input, then complex stiffness matrix of piezoelectric damper, ${}^{RE}Y$ is [11]:

$$^{RE}Y = [\,_{E}s - \hat{\imath}\omega . d^{T} . l^{-1}\,{}^{RE}Z . A . d]^{-1}; \qquad (4)$$

where: $_{E}s$ is the compliance matrix for the piezoelectric material, where the electrical field is constant (6x6 components), $\hat{\imath}$ – imaginary unit; $\omega$ – circular frequency; $l$ – diagonal matrix for electrode length (3x3 components), $d$ – matrix for piezoelectric material constants (3x6 components), $A$ is the matrix of the surface areas of piezoelectric material; and $d^{T}$ denotes transpose of a matrix.

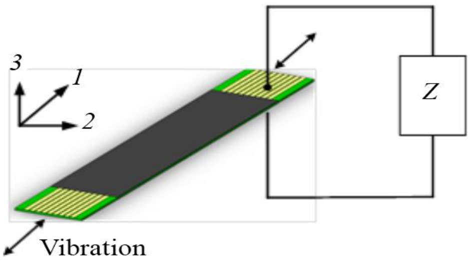


Fig. 2 PZT connected with shunted impedance

Figure 3 shows piezoelectric shunt damper with a shunt circuit, where resistor and inductor are shunted in the poling direction of piezoelectric material (direction *3*).

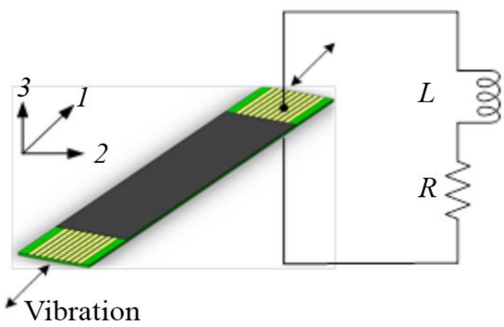


Fig. 3 PZT shunted using resistor $R$ and inductor L

The relevant component of overall impedance ${}^{RE}_{33}Z$ is given as follow [11]:

$${}^{RE}_{33}Z = \frac{1}{\left(\frac{R}{R^2+\omega^2.L^2}\right)^2 + \left(\omega.C_{P,3} - \frac{\omega.L}{(R^2+\omega^2L^2)}\right)^2} \times \left(\left(\frac{R}{R^2+\omega^2.L^2}\right)^2 - \hat{\imath}\left(\omega.C_{P,3} - \frac{\omega.L}{(R^2+\omega^2L^2)}\right)^2\right); \qquad (5)$$

where $R$ and $L$ denotes the resistance and inductance of the circuit respectively and $C_{P,3}$ is the capacitance of the piezoelectric material, where stress is constant for direction *3* [10]. The strained direction for piezo material is in the direction *1*, the relevant stiffness component of a piezoelectric damper is [11]:

$${}^{RE}_{11}Y = {}^{E}_{11}Y \times \frac{1}{\left(1 - \frac{\omega.C_{p,3}.k_{31}{}^2.\left(\omega.C_{p,3} - \frac{\omega.L}{R^2+\omega^2.L^2}\right)}{\left(\frac{R}{R^2+\omega^2.L^2}\right)+\left(\omega.C_{p,3} - \frac{\omega.L}{R^2+\omega^2.L^2}\right)}\right)^2 + \left(\frac{\omega.C_{p,3}.k_{31}{}^2.c_{LR}}{c_{LR}+d_{LR}}\right)^2} \times \left(\left(1 - \frac{\omega.C_{p,3}.k_{31}{}^2.\left(\omega.C_{p,3} - \frac{\omega.L}{R^2+\omega^2.L^2}\right)}{\left(\frac{R}{R^2+\omega^2.L^2}\right)+\left(\omega.C_{p,3} - \frac{\omega.L}{R^2+\omega^2.L^2}\right)}\right) + \hat{\imath}.\left(\frac{\omega.C_{p,3}.k_{31}{}^2.\left(\frac{R}{R^2+\omega^2.L^2}\right)}{\left(\frac{R}{R^2+\omega^2.L^2}\right)+\left(\omega.C_{p,3} - \frac{\omega.L}{R^2+\omega^2.L^2}\right)}\right)\right); \qquad (6)$$

where $k_{31}$ and ${}^{E}_{11}Y$ are electromechanical coupling coefficient and Young's modulus, respectively, for a piezoelectric material, where electric field is constant. The damping factor $\beta$ is obtained from the phase angle for the imaginary and real parts of ${}^{RE}_{11}Y$[11]:

$$\beta = \sin\left(\frac{1}{2}.\tan^{-1}\frac{\mathbf{Im}({}^{RE}_{11}Y)}{\mathbf{Re}({}^{RE}_{11}Y)}\right). \qquad (7)$$

## 4 Existing Methods of Using Piezoelectric Patches as Vibration Dampers

In a piezoelectric damper the mechanical energy associated with vibration is dissipated by transforming mechanical energy to electrical energy and followed by generating heat energy by providing shunt circuits.

Figure 4 shows the schematic representation of passive shunt damper. Passive shunt damper consist of a PZT patched on a vibrating beam and the capacitance of PZT patch, which is connected in series with resistor $R$ and inductance $L$ by forming a shunt circuit. Here optimal damping is obtained by tuning the electrical resonance based on the frequency of the chosen structural mode.

Passive damping technique can be more easily integrated because of their simplicity and compactness.


Fig. 4 Schematic of passive shunt dampers

The schematic representation of active controllable damper using piezoelectric patch is shown in Fig. 5. The active system consists of piezoelectric patches in the form of sensors and actuators, which are connected to each other through a control system. Signals obtained from sensors are filtered and used for communication with control system. At a specific amplitude of vibration, the control system will activate the actuator, thereby providing the required damping effect for the cantilever beam.

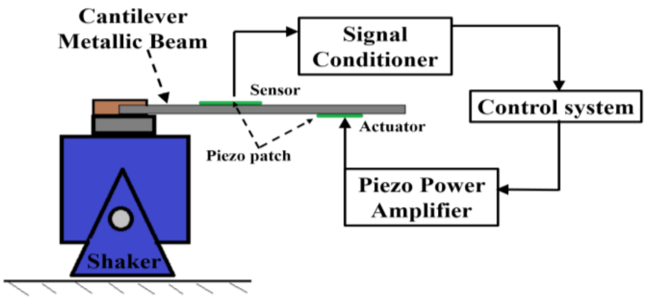


Fig. 5 Schematic of an active controlable damper

## 5 Experimental Setup and Results

For experimental setup a parallel bimorph is used with dimensions: width – 7.2 mm, thickness – 0.78 mm, total length – 40.5 mm, in which clamping area consist of 5 mm and suspended part consist of 36.5mm (Fig. 6). Figure 6 (a) shows the schematics of bimorph layers with respective attached terminals. Terminals *A* and *B* are attached to upper layer and bottom layer, which are active layers. Terminal *E* is attached to the middle layer – a very fine metallic strip, which act as the ground and also gives flexural strength to bimorph. Figure 6 (b) shows the details of bimorph used for the experiment.

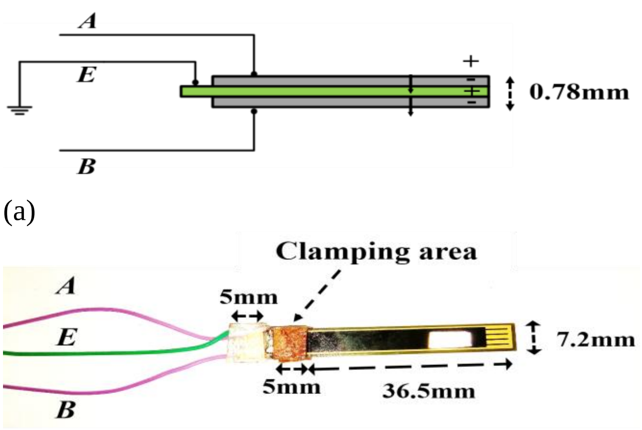


(a)

(b)

Fig. 6 Bimorph: (a) schematic of bimorph layers with respective terminals, (b) details of bimorph used for experiment

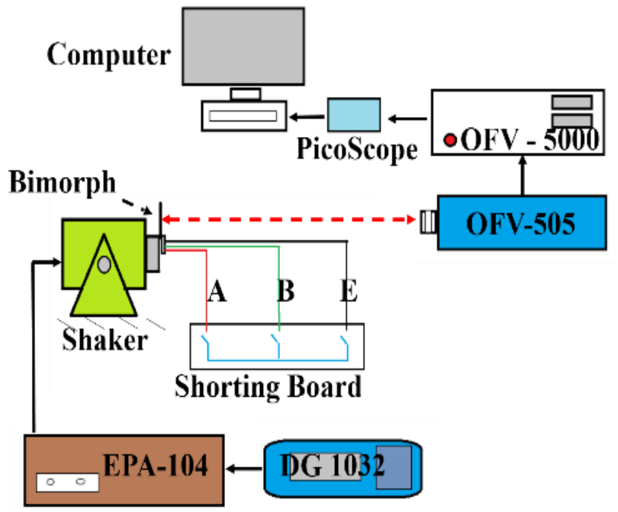


Fig. 7 Schematic of experimental setup

The schematic of experimental setup is shown Fig. 7, where a bimorph is clamped to the shaker. The shaker is excited with the help of a wave generator DG1032 and amplifier EPA-104. The amplitude of vibration transmitted to the bimorph cantilever setup is measured using optical sensor OFV-505, which is connected to a vibrometer-controller OFV-5000. The data received from vibrometer-controller OFV-5000 is analysed with the help of Pico Scope and computer.

Figure 8 shows the actual experimental setup and highlights the clamping of bimorph to shaker.

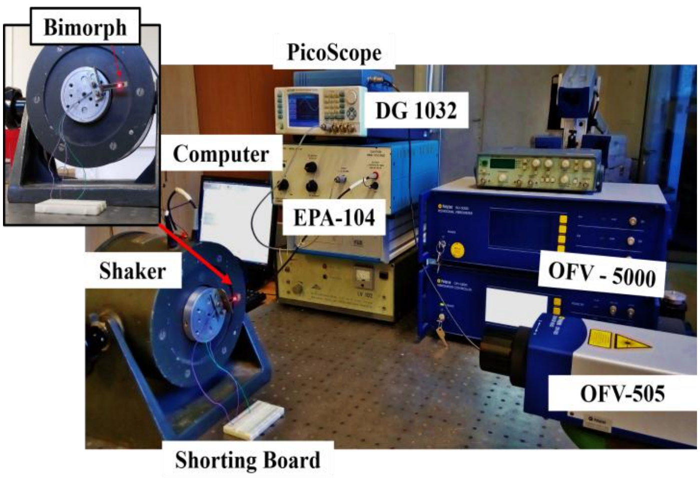


Fig. 8 Experimental setup

To analyze the nature of bimorph cantilever setup clamped to the shaker, a bump test was conducted. The damping ratio $\delta$, damping coefficient $\varsigma$ and natural frequency $f_n$, for respective combination of shortening of terminals were analyzed through bump test. From the results (Table 1) it can be observed that damping ratio, damping coefficient values and also the natural frequency varies with respect to the terminals shorted. The results obtained can be justified using equations (2) and (3), which describes that the mechanical "stiffness" of the material reduces when the output is electrically shorted.

Table 1 Results from bump test

| Nature of connection | Damping ratio $\delta$ | Damping coefficient $\varsigma$ | Natural frequency $f_n$ (Hz) |
|---|---|---|---|
| Free | 0.181 | 0.0288 | 220 |
| *A*+*B* | 0.282 | 0.0398 | 221 |
| *A*+*E* | 0.123 | 0.0196 | 213.5 |
| *B*+*E* | 0.146 | 0.0233 | 213 |
| *A*+*B*+*E* | 0.1306 | 0.0208 | 208.5 |

The bimorph was excited at frequencies equal to the natural frequency by using the shaker. The resonance characteristics that broadens the range of resonance frequency area is shown in Fig. 9. The resonance frequency when no terminals were shorted is given by $F_n$, where excitation frequency is 220 Hz and the maximum amplitude observed was 404 µm. When terminals *A* and *B* shorted the amplitude raised to 410 µm and resonance frequency $F_{n1}$ remains the same as 220 Hz. But when terminals *A* and *E* were shorted the resonance frequency changed to $F_{n2}$ – 214 Hz with a maximum amplitude 412 µm. The resonance frequency of cantilever setup again reduced to $F_{n3}$ – 213 Hz and showed a maximum amplitude as 401 µm when the terminals *B* and *E* were shorted. When all the terminals *A*, *E* and *B* were shorted together, then resonance frequency value changed to $F_{n4}$ – 208 Hz with a maximum amplitude of 397 µm.

When no terminals are connected, the natural frequency $F_n$, of the bimorph was observed at 220 Hz with a maximum amplitude of 404 µm. At 220 Hz when the terminals *A*+*E* and *B*+*E* were shorted, then maximum amplitude reduced to 300 µm. The maximum amplitude reduced to 200 µm when all the terminals *A*+*B*+*E* were shorted together. Thus, it can be stated that the reduction in amplitude is about 50 %.

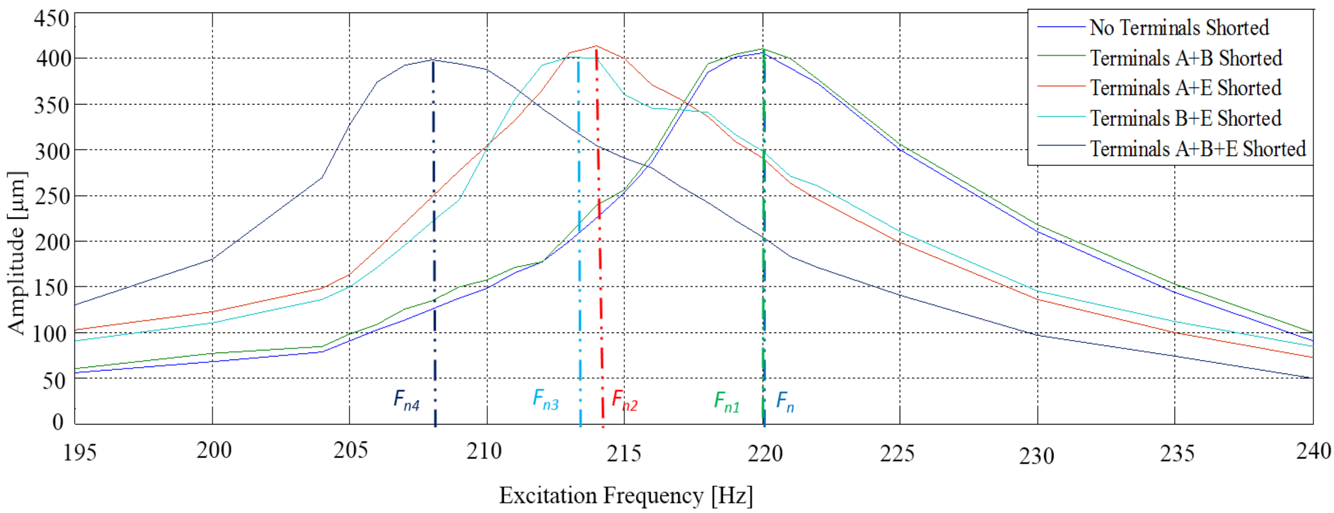


Fig. 9 Change in resonance characteristics for different combinations of terminals.

## 6 Conclusion

From the experiment it was observed, when the terminals of bimorph are shorted to each other the amplitude of vibration in the bimorph cantilever setup reduces up to 50 %. This process can explain the change in stiffness property that results in change in frequency, when the terminal are shorted to one another.

These results were achieved without providing any additional shunt circuits or external power supply. So through a proper shorting circuit and a control system, the mechanical resonance of the bimorph setup can be controlled.

This research work and its understanding is useful for providing damping at the time of resonance and for developing controllable dampers. In addition, the understanding of the research work can be applied for piezoelectric cantilever beam harvesters, which are used for harvesting energy at the time of resonance.

## Acknowledgement

Authors would like to express special token of gratitude for Professor Ramutis Petras Bansevicius and Assoc. Professor Jurenas Vytautas of Institute of Mechatronics at Kaunas University of Technology, for their valuable guidance and providing with required materials for this research work.

*References:*

[1] F. A. C. Viana and V. Steffen, Multimodal Vibration Damping through Piezoelectric Patches and optimal Resonant Shunt Circuits, *Journal of the Brazilian Society of Mechanical Sciences and Engineering*, Vol.28, No.3,pp.293-210.

[2] Inderjit Chopra, Review of State of Art of Smart Structures and Integrated Systems, *AIAA JOURNAL*, Vol. 40, No. 11, 2002

[3] Moheimani, S, A Survey of Recent Innovations in Vibration Damping and Control Using Shunted Piezoelectric Transducers *IEEE Transaction on Control Systems Technology*, 11(4), 2003, 482–494.

[4] N. W. Hagood, A. Von Flotow, Damping of Structural Vibrations with Piezoelectric Materials and Passive Electrical Networks, *J. of Sound and* Vibration, 146(2),199, 1243-268.

[5] Davis, C.L., and Lesieutre, G.A, A Modal Strain Energy Approach to the Prediction of Resistively Shunted Piezoceramic Damping, *Journal of Sound and Vibration*, Vol. 184, No.1, 1995, pp.129-39,

[6] J. B. Min, K. P. Duffy, B. B. Choi, C. R. Morrison, R. H. Jansen, A. J. Provenza, A Resonant Damping Study Using Piezoelectric Materials. *NASA Glenn Research Center Cleveland*.

[7] K. Uchino, *Piezoelectric/Electrostrictive Actuators*, Morikita Publishing, Tokyo, 1986.

[8] T. Ikeda, *Fundamentals of Piezoelectric Materials Science*, Ohm Publishing Co, Tokyo, 1984.

[9] S. Roundy ; E.S. Leland ; J. Baker ; E. Carleton ; E. Reilly ; E. Lai ; B. Otis ; J.M. Rabaey ; P.K. Wright ; V. Sundararajan, Improving power output for vibration-based energy scavengers, *IEEE Trans. Pervasive Computing,* Vol. 4, No1,pp.28-36

[10] J. Ajitsaria, S. Y. Choe, D. Shen and D. J. Kim, Modeling and analysis of a bimorph piezoelectric cantilever beam for voltage generation, *SMART MATERIALS AND STRUCTURES,* Vol.16, No. 2,pp. 447–454

[11] Y. Kitagawa, H. Tamai And M. Takeshita, Characteristics of piezoelectric dampers and their application to tall buildings as a smart structural system, *13th World Conference on Earthquake Engineering* Vancouver, B.C., Canada, August 1-6, 2004 Paper No. 1885